IRANIAN JOURNAL OF CATALYSIS

IJC
Iranian Journal of Catalysis

Surface modification of γ-alumina by NaNO₂, NaNO₃, HNO₂, HNO₃ and H₂SO₄: A DFT-D approach

Mehdi Zamani[a],*, Hossein A. Dabbagh[b]

[a]*School of Chemistry, Damghan University, Damghan 36716-41167, Iran.*
[b]*Department of Chemistry, Isfahan University of Technology, Isfahan 84156-83111, Iran.*

ABSTRACT

In this study, the dissociative adsorption of NaNO₂, NaNO₃, HNO₂, HNO₃ and H₂SO₄ over (1 1 0) surface of γ-alumina non-spinel model were investigated through the dispersion corrected density functional theory (DFT-D) at PBE-D/DNP level of calculation. It was found that all of the species are dissociated to their ionic forms after adsorption and relaxation over the surface, i.e. $Na^+NO_2^-$, $Na^+NO_3^-$, $H^+NO_2^-$, $H^+NO_3^-$, $H^+HSO_4^-$ and $2H^+SO_4^{2-}$. The Lewis acidity of alumina surface by addition of HNO₂, HNO₃ and H₂SO₄ is increased, while in the presence of NaNO₂ and NaNO₃, the acidity of catalyst is decreased. Theoretical calculations predict stronger dissociative adsorption of H₂SO₄ over the surface in compared to other compounds. The HNO₂ and HNO₃ mineral acids are better adsorbed over the surface than NaNO₂ and NaNO₃ salts. The better adsorption of nitrites than nitrates is due to the stronger electrostatic attractions. The order of NaNO₃ < NaNO₂ < HNO₃ < HNO₂ < H₂SO₄ for the dissociative adsorption energy of the title compounds is predicted.

Keywords: γ-Alumina, Surface, Adsorption, Dissociation, DFT, DOS.

1. Introduction

γ-Alumina is familiar catalyst with both acidic and basic properties. Studying the structure, reactivity and selectivity of this compound, especially at nanoscale, via experimental and theoretical methods has been of great interest over the recent years [1-23]. Theoretical studies of the adsorption on γ-alumina have focused generally on Lewis acidity of the surface [1-4], and the reactivity with H₂O [5-11], H₂S [5,10,12], CO [5,10,13], NH₃ [6], pyridine [4,6], HCl [7], alkenes [14,15], alkanes [16], alcohols [17-24] and ethers [23].

The aluminum surface sites of γ-alumina can be classified into two categories. The first one contains the tri- and tetra-coordinated aluminum sites present on the (1 1 0) surface. The second one consists of the penta-coordinated aluminum sites present on the (1 0 0) surface. It is well-known that the (1 1 0) surface is the most active plane of γ-alumina [5]. The tri-coordinated aluminum sites of the alumina surface are the dissociative sites for H₂O and H₂S molecules [5].

The tetra-coordinated aluminum sites are the non-dissociative adsorption sites for H₂O molecule, while these sites are dissociative for H₂S [5]. The penta-coordinated aluminum sites are the non-dissociative sites for H₂O and H₂S molecules [5]. The interaction of HCl molecule to the aluminum Lewis sites of γ-alumina can be either associative adsorption to Al-sites or dissociative adsorption to Al-O-sites [7]. The adsorption of alcohols over the Al sites of γ-alumina is both non-dissociative [18] and dissociative [22]. The tertiary alcohols are better adsorbed over the surface than secondary and primary alcohols [24]. The alcohols with larger alkyl chains have greater adsorption energies [24]. Also, the aryl alcohols are adsorbed over the surface better than the alkyl and allyl moieties [24]. The mechanisms of adsorption, dissociation, dehydration and dehydrogenation of alcohols over γ-alumina surface are fully discussed by the present authors [19,20].

The quantum chemical studies have recently predicted some novel models of γ-alumina based on the cluster model [5,12,14,16,17,25-27] or periodic slab on the surface [4,10,12,28-37]. For example, Sohlberg et al. reported the presence of various amounts of hydrogen

*Corresponding author email: m.zamani@du.ac.ir
Tel: +98 23 3522 0095; Fax: +98 23 3522 0095

inside the bulk structure of spinel γ-alumina [25]. They proposed that γ-alumina is a sequence of hydrogen-containing compounds. Wolverton and Hass [38] indicated that hydrogen spinel is thermodynamically unstable with respect to decomposition into an anhydrous defect spinel plus boehmite. Raybaud and co-workers reported a complete non-spinel structure based on molecular dynamic simulations and DFT calculations of the dehydration of boehmite [4,29-33]. This model showed good agreement with experimental data in terms of structural parameters and OH vibrational frequencies. Also, Paglia et al. [39,40] illustrated that the non-spinel structure of γ-alumina matches data from neutron diffraction experiments. The single crystal X-ray diffraction model of γ-alumina indicates that, in addition to the ideal spinel positions, approximately 6% of Al ions also occupy non-spinel positions [41].

γ-Alumina is generally produced by calcination of aluminum oxy-hydroxide at 350-700°C [42]. Sometimes, the mineral acids such as HNO_3 and H_2SO_4 are added during the preparation method to catalyze the hydrolysis and gelation reactions, control the particle size distribution, and improve the acidity, specific surface area and catalytic activity of γ-alumina [43]. Sulfated alumina compounds are well-known solid-acid catalysts. They can be prepared by exposing γ-alumina to H_2SO_4 followed by calcination [44]. There is no theoretical report in the literature about the bonding nature and surface modification of γ-alumina by minerals, namely, $NaNO_2$, $NaNO_3$, HNO_2, HNO_3 and H_2SO_4, which is the subject of the present study.

2. Computation

The (1 1 0) surface orientation from non-spinel model of γ-alumina [29-33] was cleaved. This model is widely used in the literature for analyzing the adsorbed species.

A vacuum of 15 Å between slabs in the direction of the crystal lattice, perpendicular to the surface plane, and periodically repeated unit cell through space was imposed. All of the possible orientations for adsorption of $NaNO_2$, $NaNO_3$, HNO_2, HNO_3 and H_2SO_4 species over this surface were examined using condensed-phase optimized molecular potentials for atomistic simulation studies (COMPASS) force field [45]. Only the energetically more favorable structures were selected for further investigations through dispersion corrected density functional theory (DFT-D) using Grimme procedure [46]. The global energy minimum structures were optimized by PBE-D method and the numerical basis set of double-zeta plus polarization quality (DNP) [47,48]. For all calculations, the integration accuracy, the self-consistent field (SCF) tolerance and the orbital cutoff quality were set to fine. Also, the effective core potentials (ECP) were used to treat the core electrons. It was found that all of the species are dissociated to their ionic forms after adsorption and relaxation over the surface, namely, $Na^+NO_2^-$, $Na^+NO_3^-$, $H^+NO_2^-$, $H^+NO_3^-$, $H^+HSO_4^-$ and $2H^+SO_4^{2-}$ (Scheme 1). The dissociative adsorption energy (ΔE) of these compounds over γ-alumina (1 1 0) surface was calculated by eq. (1), where $E_{(adsorbed\ species\ on\ surface)}$, $E_{(species)}$ and $E_{(surface)}$ refer to the energy of the system after dissociative adsorption, energy of isolated species and energy of bare alumina surface, respectively.

$$\Delta E = E_{(adsorbed\ species\ on\ surface)} - (E_{(species)} + E_{(surface)}) \quad (1)$$

The bonding nature of these compounds over γ-alumina (1 1 0) surface was analyzed by the calculation of density of state (DOS) diagrams, and by the decomposition of ΔE to its components (the sum of atomic energies, kinetic, electrostatic, exchange-correlation, spin polarization and dispersion energy). All calculations were performed using the $DMOL^3$ program [47,48].
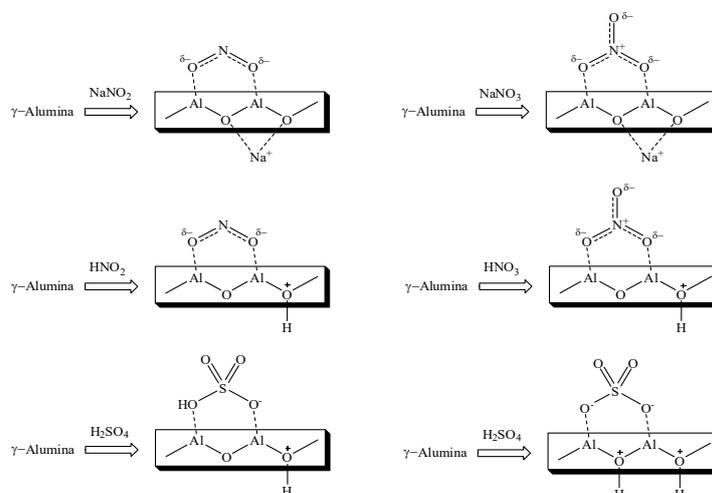
Scheme 1. The dissociative adsorption of $NaNO_2$, $NaNO_3$, HNO_2, HNO_3 and H_2SO_4 over γ-alumina.

3. Results and Discussion

It has been reported that the (1 1 0) surface of γ-alumina with 74% of total area is the most catalytically active surface of γ-alumina [31]. In this study we focused on the active sites of this surface for adsorption of minerals, namely, $NaNO_2$, $NaNO_3$, HNO_2, HNO_3 and H_2SO_4. Fig. 1 shows the optimized geometry of this surface calculated at BPE-D/DNP level of theory. The top layers of this surface (ball & stick model) were fully optimized, while the position of atoms in bottom layers was kept fixed (stick model). The upper layer of this surface is composed from four aluminums (Al_{1-4}) and six oxygen (O_{1-6}) atoms, which acts as Lewis acid and Brønsted basic sites, respectively. These sites have an important role in the catalytic activity of γ-alumina. The calculated bond lengths and Mulliken atomic charges for these sites are listed in Table 1. According to these results, the maximum value of positive charge is located on the tri-coordinated atom Al_1 with the atomic charge of 1.211 ē. This site is much stronger Lewis acid than tetra-coordinated atoms Al_{2-4} with atomic charges of 1.151, 1.151 and 1.115 ē, respectively.

The mono dentate anions (or nucleophiles) are adsorbed on the Al_1 site. Calculations showed that the global minimum structure of γ-alumina (1 1 0) surface after adsorption of ion OH^- belongs to the bonding of OH^- with Al_1 at the equilibrium distance of 1.752 Å (Fig. 2a). Analysis of the atomic charges of this structure (Table 1) shows that the adsorption of OH^- over the γ-alumina (1 1 0) surface reduces the positive charges of Lewis acid sites Al_{1-4}. The Mulliken atomic

charges for basic sites O_{1-6} were calculated in the range of −0.775 to −0.877 ē. The tri-coordinated atoms $O_{3, 4, 6}$ have larger values of negative charge (−0.877, −0.877 and −0.864 ē) than di-coordinated sites $O_{1, 2, 5}$ (−0.775, −0.775 and −0.784 ē), but the latter sites are more reactive for abstraction of H^+. The global minimum structure of γ-alumina (1 1 0) surface after adsorption of ion H^+ corresponds to the bonding of H^+ with O_5 at distance of 1.040 Å (Fig. 2b). The stability of this structure is the result of intramolecular hydrogen bond (1.565 Å) between γ-alumina O_1 site and adsorbed H atom. The global minimum structure of γ-alumina (1 1 0) surface after adsorption of $2H^+$ is shown in Fig. 2c. The secondary H^+ is bonded to site O_5 at distance of 0.977 Å. Analysis of the calculated atomic charges of γ-alumina (1 1 0) surface after adsorption of H^+ and $2H^+$ in comparison to pure surface reveals that the positive charge of Lewis acid sites alumina is increased. For example, the charge of Al_1 from 1.211 ē for the pure surface is increased to 1.309 and 1.328 ē after adsorption of H^+ and $2H^+$ on the surface, respectively.

Fig. 3 shows the partial density of states (PDOS) of γ-alumina (1 1 0) surface bonded with OH^-, H^+ and $2H^+$ in comparison to the pure surface. To focus on the bonding nature of these species, only the valence band is shown in these Figs. The position of Fermi level is 0 eV. The conduction band appears at the larger positive energies. The lower valence band of alumina (−21 to −15 eV) is mainly composed from O *2s* orbitals, while the upper valence band (−9 to 0 eV) is mainly consisting of O *2p* orbitals, which slightly overlaps with Al *3s* and Al *3p* orbitals (Fig. 3a).
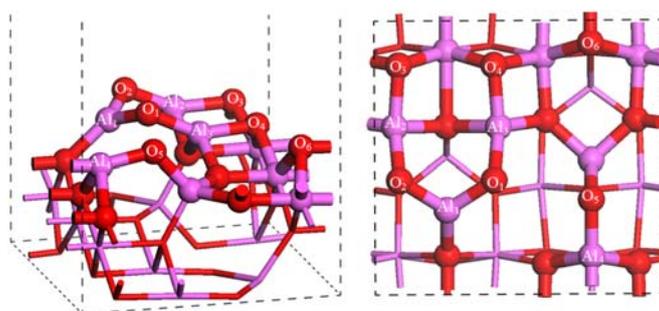

Fig. 1. Optimized structure of γ-alumina (1 1 0) surface calculated by BPE-D/DNP level of theory; side view (left), top view (right).
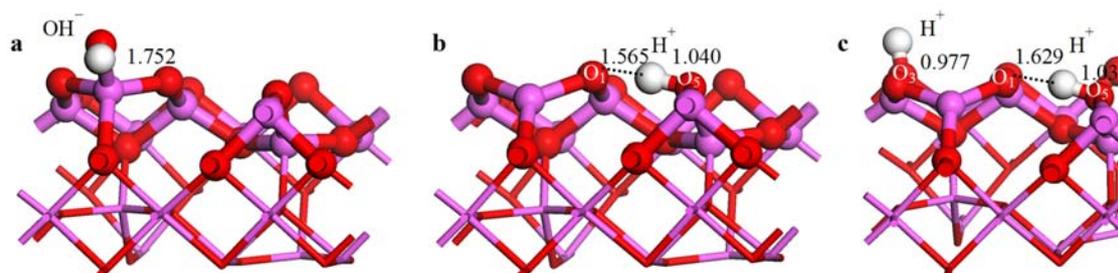

Fig. 2. The global minimum structures of γ-alumina (1 1 0) surface after bonding with OH^- (a), H^+ (b) and $2H^+$ (c) calculated by BPE-D/DNP level of theory.

Table 1. Bond lengths (Å) and partial atomic charges of γ-alumina (1 1 0) surface before and after bonding with various studied species.

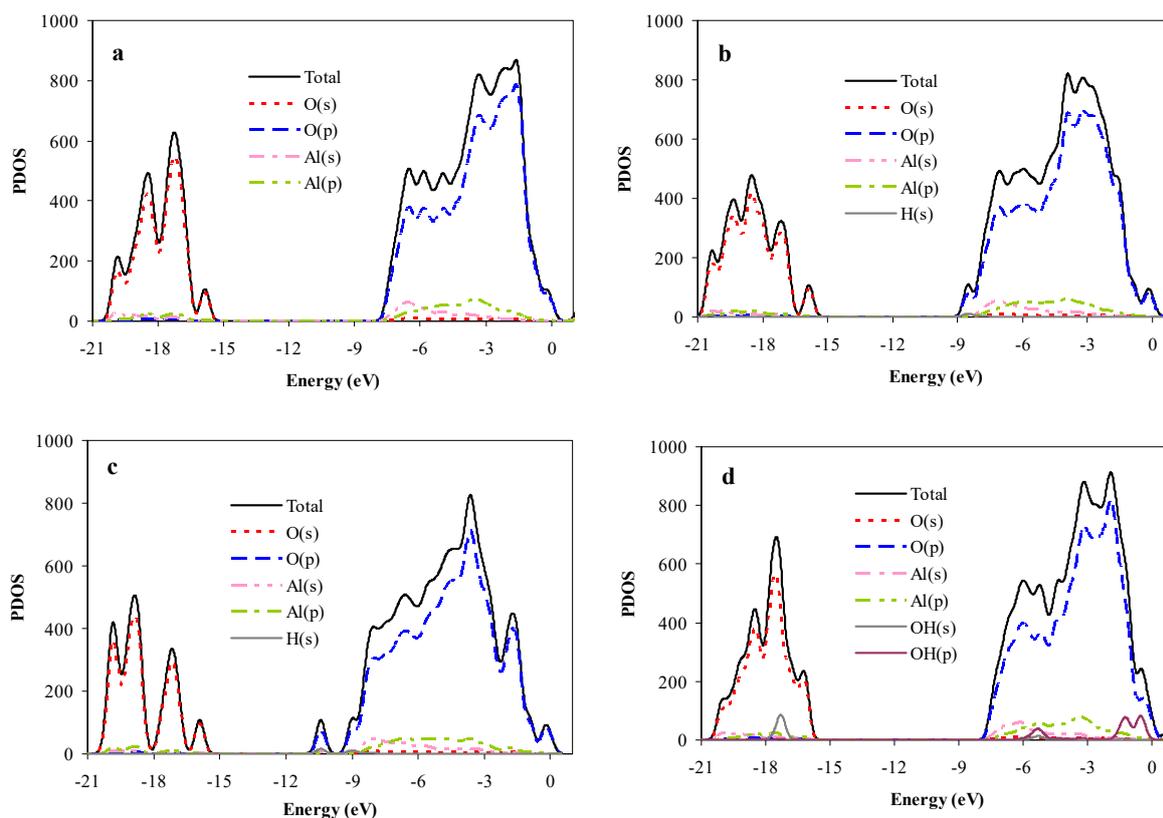| Entry	Pure (1 1 0) surface	(1 1 0) Surface modified by										
		OH^- (Fig. 2a)	H^+ (Fig. 2b)	$2H^+$ (Fig. 2c)	Na^+ (Fig. 4a)	$Na^+NO_2^-$ (Fig. 4b)	$Na^+NO_3^-$ (Fig. 4c)	$H^+NO_2^-$ (Fig. 4d)	$H^+NO_3^-$ (Fig. 4e)	$H^+HSO_4^-$ (Fig. 4f)	$H^+SO_4^{2-}$ (Fig. 4g)	$2H^+SO_4^{2-}$ (Fig. 4h)
Bond Lengths												
Al_1-O_1	1.726	1.784	1.765	1.750	1.791	1.798	1.794	1.799	1.792	1.790	1.798	1.793
Al_1-O_2	1.726	1.784	1.728	1.728	1.751	1.763	1.762	1.765	1.764	1.767	1.773	1.775
Al_2-O_2	1.745	1.711	1.752	1.719	1.752	1.742	1.744	1.743	1.744	1.742	1.734	1.700
Al_2-O_3	1.844	1.860	1.837	1.998	1.828	1.861	1.859	1.859	1.859	1.867	1.855	2.051
Al_3-O_1	1.745	1.709	1.786	1.774	1.771	1.728	1.728	1.745	1.741	1.736	1.734	1.730
Al_3-O_4	1.844	1.861	1.818	1.818	1.812	1.809	1.811	1.808	1.811	1.855	1.803	1.803
Al_4-O_5	1.716	1.715	1.825	1.828	1.744	1.761	1.760	1.852	1.858	1.878	1.880	1.884
Charges												
Al_1	1.211	1.183	1.309	1.328	1.281	1.285	1.311	1.311	1.333	1.358	1.312	1.345
Al_2	1.151	1.117	1.182	1.272	1.162	1.133	1.137	1.156	1.159	1.157	1.143	1.219
Al_3	1.151	1.118	1.204	1.214	1.253	1.234	1.250	1.168	1.183	1.219	1.180	1.183
Al_4	1.115	1.116	1.201	1.226	1.188	1.294	1.302	1.278	1.290	1.313	1.295	1.303
O_1	−0.775	−0.800	−0.890	−0.875	−0.896	−0.909	−0.909	−0.901	−0.897	−0.890	−0.902	−0.891
O_2	−0.775	−0.802	−0.787	−0.763	−0.776	−0.808	−0.808	−0.818	−0.819	−0.816	−0.827	−0.796
O_3	−0.877	−0.891	−0.868	−0.788	−0.873	−0.875	−0.875	−0.882	−0.881	−0.880	−0.886	−0.814
O_4	−0.877	−0.902	−0.863	−0.854	−0.871	−0.879	−0.895	−0.879	−0.897	−0.977	−0.865	−0.857
O_5	−0.784	−0.785	−0.798	−0.785	−0.900	−0.914	−0.913	−0.819	−0.815	−0.799	−0.808	−0.797
O_6	−0.864	−0.872	−0.843	−0.840	−0.853	−0.865	−0.867	−0.866	−0.868	−0.871	−0.877	−0.872

Fig. 3. The calculated partially density of states (PDOS) for the global minimum structures of γ-alumina (1 1 0) surface before (a), and after bonding with H^+ (b), $2H^+$ (c) and OH^- (d).

Since the contribution of Al orbitals in the valence band cannot be ignored, Digne et al. concluded that the Al–O bonds in γ-alumina tends to be rather ionocovalent than purely ionic [31]. As shown in Fig. 3b-d that PDOS of γ-alumina (1 1 0) surface after adsorption of H^+, $2H^+$ and OH^- has been dramatically changed (due to covalent nature of these bonds and the geometry relaxation of the surface). The hydrogen $1s$ state for the adsorbed H^+ appears almost at −8.3 eV (Fig. 3b).

Similar states corresponding to the adsorbed $2H^+$ surface are seen at −8.8 and −10.2 eV (Fig. 3c). The position of the states due to s and p orbitals of OH^- is found in the middle of lower valence band (at −17.2 eV) and in conjugation with the upper valence band of γ-alumina, i.e. −5.1, −1.1 and −0.4 eV (Fig. 3d).

The global minimum structures of γ-alumina (1 1 0) surface after adsorption of $NaNO_2$, $NaNO_3$, HNO_2, HNO_3 and H_2SO_4, calculated by BPE-D/DNP level of theory are shown in Fig. 4. It was found that all of these compounds are dissociated to their ionic forms after adsorption and relaxation over the surface, i.e. $Na^+NO_2^-$, $Na^+NO_3^-$, $H^+NO_2^-$, $H^+NO_3^-$, $H^+HSO_4^-$ and $2H^+SO_4^{2-}$. PDOS diagrams are indicated in Fig. 5.

The calculated binding energies and their components are listed in Table 2. As seen in Fig. 4a that Na^+ adsorbs in an interstitial position with the equilibrium distances of 2.232 and 2.251 Å from the sites of O_1 and O_5 of alumina surface, respectively.

Based on the results of Table 1, the Lewis acidity of surface after modification by Na^+ is slightly increased (promotion of the positive charges). The adsorbed Na cation is carrying the positive charge of 0.756 ē, while the corresponding value for H^+ is 0.415 ē. Therefore, the effect of Na^+ on the improvement of the Lewis acidity of alumina surface is weaker than H^+. According to the atomic charges listed on Table 1, the Lewis acidity of alumina surface by addition of HNO_2, HNO_3 and H_2SO_4 has been increased. While in the presence of $NaNO_2$ and $NaNO_3$, the acidity of the catalyst has been decreased.

Fig. 4b-h shows that all of the anionic species of NO_2^-, NO_3^-, HSO_4^- and SO_4^{2-} interact interstitial with both Al_1 and Al_4 sites of γ-alumina (1 1 0) surface. The bond distance between oxygen atoms of NO_2^- from Al_1 and Al_4 sites of alumina surface modified by H^+ is 1.898 and 1.969 Å, respectively (Fig. 4d). These distances for modified alumina surface by Na^+ (Fig. 4b) are longer (1.923 and 2.140 Å, respectively).
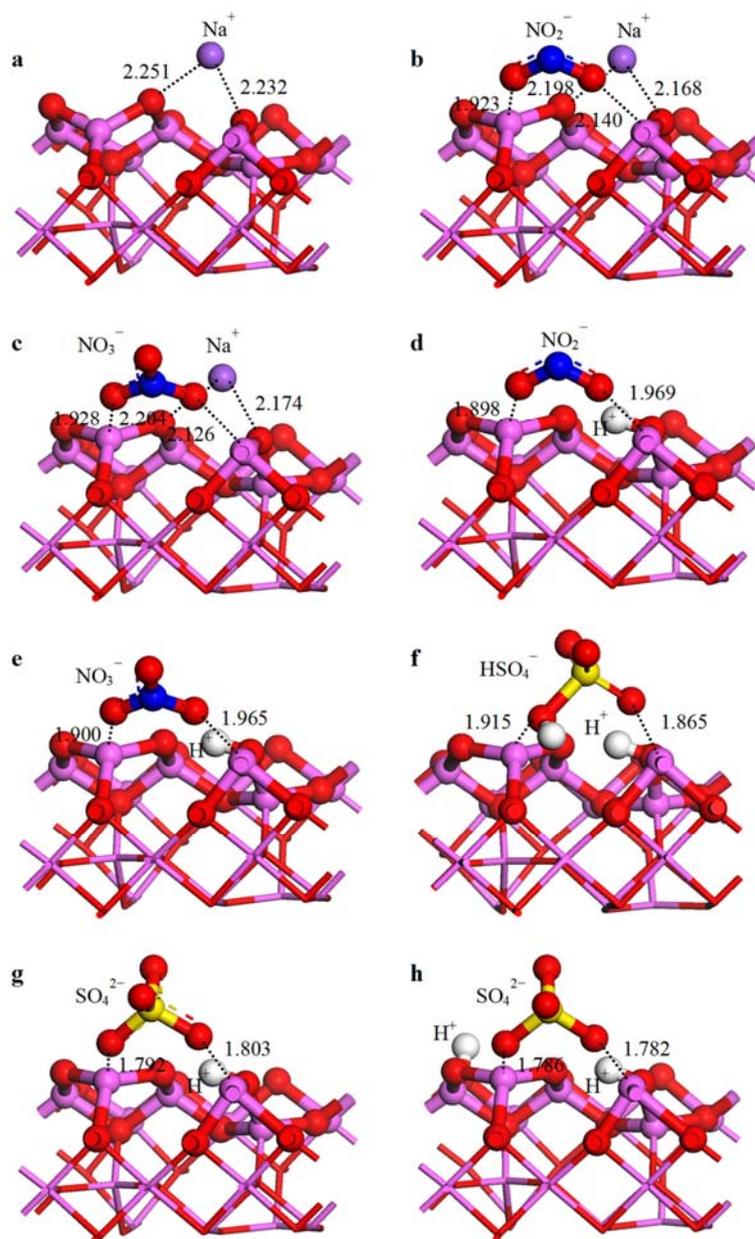
Fig. 4. The global minimum structures of γ-alumina (1 1 0) surface after bonding with Na^+ (a), $Na^+NO_2^-$ (b), $Na^+NO_3^-$ (c), $H^+NO_2^-$ (d), $H^+NO_3^-$ (e), $H^+HSO_4^-$ (f), $H^+SO_4^{2-}$ (g) and $2H^+SO_4^{2-}$ (h).

Similar results are achieved for adsorption of NO_3^- over the modified alumina surfaces, i.e. 1.900, 1.928 Å (Fig. 4e) vs. 1.928, 2.174 Å (Fig. 4c). The minimum distances from the surface was predicted for sulfate ion (1.786 and 1.782 Å), Fig. 4g, h. In the case of HSO_4^-, the bond distances from the surface are longer (1.915, 1.865 Å) (Fig. 4f).

The highly accurate dissociation energy of HNO_2 and HNO_3 to ions H^+, NO_2^- and NO_3^- is estimated via CBS-QB3 method as 14.72 and 14.03 eV, respectively (endothermic). The dissociative adsorption of these molecules over (1 1 0) surface of γ-alumina

(after binding to the surface and surface relaxation) is an exothermic process with −18.36 and −17.83 eV energy release, respectively (Scheme 1).

The corresponding values for the dissociation and bonding of $NaNO_2$ and $NaNO_3$ over (1 1 0) surface of γ-alumina are −9.93 and −9.48 eV, respectively. Therefore, the HNO_2 and HNO_3 mineral acids are better adsorbed over the surface than $NaNO_2$ and $NaNO_3$ salts. Stronger adsorption of nitrites (HNO_2 and $NaNO_2$) than nitrates (HNO_3 and $NaNO_3$) is due to more negative electrostatic part of binding energy for the former compounds (Table 2).
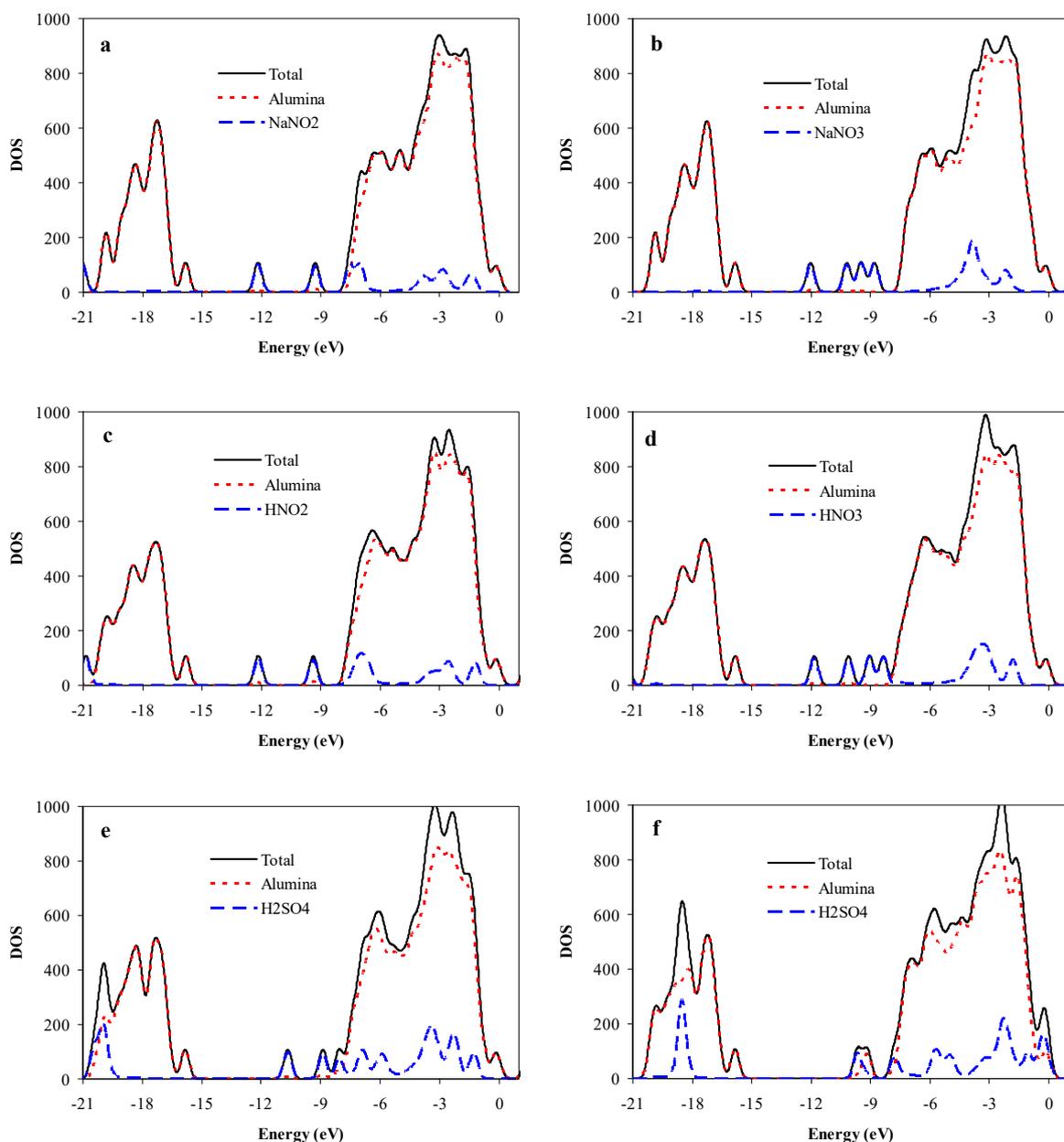
Fig. 5. The calculated density of states (DOS) for the global minimum structures of γ-alumina (1 1 0) surface after bonding with $Na^+NO_2^-$ (a), $Na^+NO_3^-$ (b), $H^+NO_2^-$ (c), $H^+NO_3^-$ (d), $H^+HSO_4^-$ (e) and $2H^+SO_4^{2-}$ (f).

The accurate value of dissociation energy for H_2SO_4 to ion pairs $H^+HSO_4^-$ and $2H^+SO_4^{2-}$ is predicted to be 13.49 and 32.92 eV via CBS-QB3 method, respectively (endothermic). The dissociative adsorption of H_2SO_4 over γ-alumina (1 1 0) surface (after binding to the surface and surface relaxation) is an exothermic process with -37.73 eV energy release. According to the results of Table 2, the following order for the dissociative adsorption energy of studied compounds over γ-alumina (1 1 0) surface is predicted: $NaNO_3$ < $NaNO_2$ < HNO_3 < HNO_2 < H_2SO_4.

4. Conclusions

In this study, the surface modification γ-alumina by $NaNO_2$, $NaNO_3$, HNO_2, HNO_3 and H_2SO_4 was investigated through the dispersion corrected density functional theory. These species are dissociated to their ionic forms after adsorption over the surface. The positive charge of Lewis acid sites of alumina was increased by surface modification with mineral acids. The Lewis acidity of alumina surface by addition of HNO_3 and H_2SO_4 is increased, while in the presence of $NaNO_2$, the acidity of catalyst is decreased.

Table 2. Theoretical estimation of ΔE and its components (eV) for the dissociative adsorption of $NaNO_2$, $NaNO_3$, HNO_2, HNO_3 and H_2SO_4 over γ-alumina (1 1 0) surface.

Adsorbent	Sum of atomic energies	Kinetic	Electrostatic	Exchange-correlation	Spin polarization	Dispersion	Dissociative adsorption energy
$Na^+NO_2^-$	−0.48	36.03	−45.77	2.44	−1.51	−0.64	−9.93
$Na^+NO_3^-$	−0.50	−18.05	8.78	2.58	−1.59	−0.69	−9.48
$H^+NO_2^-$	−0.10	−304.14	284.26	2.46	−0.43	−0.42	−18.36
$H^+NO_3^-$	−0.12	−348.03	328.69	2.60	−0.50	−0.48	−17.83
$2H^+SO_4^{2-}$	−0.12	−946.08	905.56	4.02	−0.47	−0.65	−37.73

Theoretical calculations predict stronger dissociative adsorption of H_2SO_4 over the surface in compared to other compounds. This is in agreement with the experimental data which predicted higher reactivity for γ-alumina modified by H_2SO_4. The mineral acids of HNO_2 and HNO_3 are better adsorbed over the surface than salts of $NaNO_2$ and $NaNO_3$. Stronger adsorption of nitrite compounds (HNO_2 and $NaNO_2$) than nitrates (HNO_3 and $NaNO_3$) is due to more negative electrostatic part of binding energy. The following energy order for the dissociative adsorption of title compounds is predicted: $NaNO_3$ < $NaNO_2$ < HNO3 < HNO_2 < H_2SO_4.

Acknowledgment

References

[1] H. Tachikawa, T. Tsuchida, J. Mol. Catal. A: Chem. 96 (1995) 277-282.
[2] M.B. Fleisher, L.O. Golender, M.V. Shimanskaya, J. Chem. Soc. Faraday Trans. 87 (1991) 745-748.
[3] H. Kawakami, S. Yoshida, J. Chem. Soc. Faraday Trans. 81 (1985) 1117-1127.
[4] M. Digne, P. Raybaud, H. Toulhoat, J. Catal. 226 (2004) 54-68.
[5] O. Maresca, A. Allouche, J.P. Aycard, M. Rajzmann, S. Clemendot, F. Hutschka, J. Mol. Struct. Theochem 505 (2000) 81-94.
[6] P. Hirva, T.A. Pakkanen, Surf. Sci. 277 (1992) 389-394.
[7] M. Lindblad, T.A. Pakkanen, Surf. Sci. 286 (1993) 333-345.
[8] K.C. Hass, W.F. Schneider, A. Curioni, W. Andreoni, Science 282 (1998) 265-268.
[9] J. Fernandez Sanz, H. Rabaa, F.M. Poveda, A.M. Marquez, C. Calzado, J. Int. J. Quantum Chem. 70 (1998) 359-365.
[10] O. Maresca, A. Ionescu, A. Allouche, J.P. Aycard, M. Rajzmann, F. Hutschka, J. Mol. Struct. Theochem 620 (2003) 119-128.
[11] H.A. Dabbagh, M. Zamani, Comput. Mater. Sci. 79 (2013) 781-788.
[12] A. Ionescu, A. Allouche, J.P. Aycard, M. Rajzmann, F. Hutschka, J. Phys. Chem. B 106 (2002) 9359-9366.
[13] L. Marina, T.A. Pakkanen, Surf. Sci. 286 (1993) 333-345.
[14] S. Cai, K. Sohlberg, J. Mol. Catal. A: Chem. 248 (2006) 76-83.
[15] M.L. F.erreira, E.H. Rueda, J. Mol. Catal. A: Chem. 178 (2002) 147-160.
[16] S. Cai, V. Chihaia, K. Sohlberg, J. Mol. Catal. A: Chem. 275 (2007) 63-71.
[17] D.A. De Vito, F. Gilardoni, L. Kiwi-Minsker, P.Y. Morgantini, S. Porchet, A. Renken, J. Weber, J. Mol. Struct. Theochem 469 (1999) 7-14.
[18] S. Cai, K. Sohlberg, J. Mol. Catal. A: Chem. 193 (2003) 157-164.
[19] H.A. Dabbagh, M. Zamani, B.H. Davis, J. Mol. Catal. A: Chem. 333 (2010) 54-68.
[20] H.A. Dabbagh, K. Taban, M. Zamani, J. Mol. Catal. A: Chem. 326 (2010) 55-68.
[21] G. Feng, C. Huo, C. Deng, L. Huang, Y. Li, J. Wang, H. Jiao, J. Mol. Catal. A: Chem. 304 (2009) 58-64.
[22] Z. Zuo, W. Huang, P. Han, Z. Gao, Z. Li, Appl. Catal. A Gen. 408 (2011) 130-136.
[23] Z. Zuo, P. Han, J. Hu, W. Huang, J. Mol. Model. 18 (2012) 5107-5111.
[24] M. Zamani, H.A. Dabbagh, J. Nanoanal. 1 (2014) 21-30.
[25] K. Sohlberg, S.J. Pennycook, S.T. Pantelides, J. Am. Chem. Soc. 121 (1999) 7493-7499.
[26] A. Vijay, G. Mills, H. Metiu, J. Chem. Phys. 117 (2002) 4509.
[27] J. Handzlik, J. Ogonowski, R. Tokarz-Sobieraj, Catal. Today 101 (2005) 163-173.
[28] S. Cai, M. Caldararu, V. Chihaia, C. Munteanu, C. Hornoiu, K. Sohlberg, J. Phys. Chem. C 111 (2007) 5506-5513.
[29] X. Krokidis, P. Raybaud, A. E. Gobichon, B. Rebours, P. Euzen, H. Toulhoat, J. Phys. Chem. B 105 (2001) 5121-5130.
[30] M. Digne, P. Sautet, P. Raybaud, P. Euzen, H. Toulhoat, J. Catal. 211 (2002) 1-5.

[31] M. Digne, P. Sautet, P. Raybaud, P. Euzen, H. Toulhoat, J. Catal. 226 (2004) 54-68.

[32] M.C. Valero, P. Raybaud, P. Sautet, J. Phys. Chem. B 110 (2006) 1759-1767.

[33] M. Digne, P. Raybaud, P. Sautet, B. Rebours, H. Toulhoat, J. Phys. Chem. B 110 (2006) 20719-20720.

[34] T. Taniike, M. Tada, Y. Morikawa, T. Sasaki, Y. Iwasawa, J. Phys. Chem. B 110 (2006) 4929-4936.

[35] H.P. Pinto, R.M. Nieminen, S.D. Elliott, Phys. Rev. B 70 (2004) 125402.

[36] A. Dyan, P. Cenedese, P. Dubot, J. Phys. Chem. B 110 (2006) 10041-10050.

[37] J. Handzlik, P. Sautet, J. Catal. 256 (2008) 1-14.

[38] C. Wolverton, K.C. Hass, Phys. Rev. B 63 (2000) 024102.

[39] G. Paglia, C.E. Buckley, A.L. Rohl, B.A. Hunter, R.D. Hart, J.V. Hanna, L.T. Byrne, Phys. Rev. B 68 (2003) 144110.

[40] G. Paglia, A.L. Rohl, C.E. Buckley, G.D. Gale, Phys. Rev. B 71 (2005) 224115.

[41] L. Smrcok, V. Langer, J. Krestan, Acta Cryst. C62 (2006) i83-i84.

[42] P. Souza Santos, H. Souza Santos, S.P. Toledo, Mater. Res. Ibero-Am. J. 3 (2000) 104-112.

[43] P. Manivasakan, V. Rajendran, P.R. Rauta, B.B. Sahu, B.K. Panda, Powder Technol. 211 (2011) 77-84.

[44] M.L. Guzmán-Castillo, E. López-Salinas, J.J. Fripiat, J. Sánchez-Valente, F. Hernández-Beltrán, A. Rodríguez-Hernández, J. Navarrete-Bolaños, J. Catal. 220 (2003) 317-325.

[45] H. Sun, J. Phys. Chem. B 102 (1998) 7338-7364.

[46] S. Grimme, J. Comput. Chem. 27 (2006) 1787-1799.

[47] B. Delley, J. Chem. Phys. 92 (1990) 508-517.

[48] B. Delley, J. Chem. Phys. 113 (2000) 7756-7764.